



Alfvénic Acceleration Sustains Ganymede's Footprint Tail Aurora

J. Szalay, F. Allegrini, F. Bagenal, S. Bolton, B. Bonfond, G. Clark, J. Connerney, R. Ebert, D. Gershman, R. Giles, et al.

► To cite this version:

J. Szalay, F. Allegrini, F. Bagenal, S. Bolton, B. Bonfond, et al.. Alfvénic Acceleration Sustains Ganymede's Footprint Tail Aurora. *Geophysical Research Letters*, 2020, 47 (3), 10.1029/2019GL086527 . hal-04922109

HAL Id: hal-04922109

<https://hal.science/hal-04922109v1>

Submitted on 31 Jan 2025

HAL is a multi-disciplinary open access archive for the deposit and dissemination of scientific research documents, whether they are published or not. The documents may come from teaching and research institutions in France or abroad, or from public or private research centers.

Copyright

L'archive ouverte pluridisciplinaire **HAL**, est destinée au dépôt et à la diffusion de documents scientifiques de niveau recherche, publiés ou non, émanant des établissements d'enseignement et de recherche français ou étrangers, des laboratoires publics ou privés.

Geophysical Research Letters

RESEARCH LETTER

10.1029/2019GL086527

Key Points:

- First in situ particles and fields measurements connected to Ganymede's auroral tail are reported
- Alfvén wave activity is observed with Poynting fluxes of $\sim 100 \text{ mW/m}^2$ capable of accelerating electrons into the atmosphere
- Ganymede's footprint tail contains electron populations consistent with Alfvénic acceleration and precipitating energy fluxes of $\sim 11 \text{ mW/m}^2$

Supporting Information:

- Supporting Information S1

Correspondence to:

J. R. Szalay,
jszalay@princeton.edu

Citation:

Szalay, J. R., Allegrini, F., Bagenal, F., Bolton, S. J., Bonfond, B., Clark, G., et al. (2020). Alfvénic acceleration sustains Ganymede's footprint tail aurora. *Geophysical Research Letters*, 47, e2019GL086527. <https://doi.org/10.1029/2019GL086527>

Received 3 DEC 2019

Accepted 16 JAN 2020

Accepted article online 21 JAN 2020

Alfvénic Acceleration Sustains Ganymede's Footprint Tail Aurora

J. R. Szalay¹ , F. Allegrini^{2,3} , F. Bagenal⁴ , S. J. Bolton² , B. Bonfond⁵ , G. Clark⁶ , J. E. P. Connerney^{7,8} , R. W. Ebert^{2,3} , D. J. Gershman⁸ , R. S. Giles² , G. R. Gladstone² , T. Greathouse² , G. B. Hospodarsky⁹ , M. Imai⁹ , W. S. Kurth⁹ , S. Kotsiaros⁸ , P. Louarn¹⁰ , D. J. McComas¹ , J. Saur¹¹ , A. H. Sulaiman⁹ , and R. J. Wilson⁴

¹Department of Astrophysical Sciences, Princeton University, Princeton, NJ, USA, ²Southwest Research Institute, San Antonio, TX, USA, ³Department of Physics and Astronomy, University of Texas at San Antonio, San Antonio, TX, USA,

⁴Laboratory for Atmospheric and Space Physics, University of Colorado Boulder, Boulder, CO, USA, ⁵Space Sciences, Technologies and Astrophysics Research Institute, LPAP, Université de Liège, Liège, Belgium, ⁶Johns Hopkins University Applied Physics Laboratory, Laurel, MD, USA, ⁷Space Research Corporation, Annapolis, MD, USA, ⁸Goddard Space Flight Center, Greenbelt, MD, USA, ⁹Department of Physics and Astronomy, University of Iowa, Iowa City, IA, USA, ¹⁰Institut de Recherche en Astrophysique et Planétologie, Toulouse, France, ¹¹Institute of Geophysics and Meteorology, University of Cologne, Cologne, Germany

Abstract Integrating simultaneous in situ measurements of magnetic field fluctuations, precipitating electrons, and ultraviolet auroral emissions, we find that Alfvénic acceleration mechanisms are responsible for Ganymede's auroral footprint tail. Magnetic field perturbations exhibit enhanced Alfvénic activity with Poynting fluxes of $\sim 100 \text{ mW/m}^2$. These perturbations are capable of accelerating the observed broadband electrons with precipitating fluxes of $\sim 11 \text{ mW/m}^2$, such that Alfvénic power is transferred to electron acceleration with $\sim 10\%$ efficiency. The ultraviolet emissions are consistent with in situ electron measurements, indicating $13 \pm 3 \text{ mW/m}^2$ of precipitating electron flux. Juno crosses flux tubes with both upward and downward currents connected to the auroral tail exhibiting small-scale structure. We identify an upward electron conic in the downward current region, possibly due to acceleration by inertial Alfvén waves near the Jovian ionosphere. In concert with in situ observations at Io's footprint tail, these results suggest that Alfvénic acceleration processes are broadly applicable to magnetosphere-satellite interactions.

Plain Language Summary Jupiter's moon Ganymede interacts with the planet's rapidly rotating magnetic field, which generates an aurora in the Jovian upper atmosphere. The Juno spacecraft crossed magnetic field lines connected to this aurora. We found that a specific type of wave, similar to a wave produced when a string is plucked, is responsible for accelerating the electrons sustaining this aurora. This type of interaction between a moon and the planet it orbits is likely a common process occurring at other exoplanetary systems.

1. Introduction

Jupiter's auroral features are diverse and complex, consisting of separate emission regions linked to different locations in the magnetosphere and many different physical mechanisms (e.g., Grodent, 2015). While many of these auroral features map to broad areas in the magnetosphere, the aurorae generated by the interaction of Jupiter's rotating magnetosphere with the Galilean moons allow for a more precise determination of the auroral source regions and physical processes sustaining their aurora.

Ganymede's auroral signature was discovered in ultraviolet (UV) images of Jupiter's aurora (Clarke et al. 2002) and is observed to have multiple auroral spots downstream of its main spot, whose separation varies with Ganymede's System III longitude (Bonfond et al., 2013). A more continuous auroral tail has also been observed for Ganymede, and remote sensing observations suggest this tail is sustained by reflections of Alfvén waves generated by Ganymede's interaction with Jupiter's magnetosphere (Bonfond et al., 2017). The morphology and generation of Ganymede's auroral signatures are expected to be similar to Io's tail (Bonfond et al., 2017), such that it has a Main Alfvén Wing (MAW) spot, a transhemispheric electron beam (Bonfond et al., 2008), and a footprint tail aurora. Similar to Io, high-resolution infrared images have revealed Ganymede's tail to be highly structured (Mura et al., 2018). In situ observations by the Juno

spacecraft have bolstered the case that Alfvénic acceleration is sustaining Io's footprint tail aurora (Bonfond et al., 2009) from measurements of broadband precipitating electron fluxes (Szalay et al., 2018) and Alfvénic magnetic signatures (Gershman et al., 2019). Since our understanding of Io's auroral interaction is coalescing around a dominantly Alfvénic acceleration mechanism sustaining both the MAW and tail, and similar acceleration processes are operating at Saturn's moon Enceladus (e.g., Sulaiman et al., 2018), identifying the acceleration mechanism at another Jovian moon allows us to test the assertion that this process is more broadly applicable to moon-magnetosphere interactions as a whole (Bonfond, Grodent, et al., 2017; Bonfond, Saur, et al., 2017).

While Io's auroral signature is the best cataloged of the Galilean moons due to it being the brightest satellite interaction, Ganymede's auroral footprint characteristics have also been well-documented. Ganymede's footprint aurora varies on three different time scales, the largest corresponding to Jupiter's orbital period of ~ 10 hr, where the footprint emission is strongest when Ganymede is exposed to the largest plasma sheet densities (Grodent et al., 2009). The average emitted power of Ganymede's auroral footprint is estimated to range from 0.2–1.5 GW (Grodent et al., 2009) and 0.8–6.3 GW (Bonfond, Grodent, et al., 2017). The total theoretically calculated Poynting fluxes generated by Ganymede's interaction are estimated to lie between 1–150 GW depending on Ganymede's position in Jupiter's plasma sheet (Saur et al., 2013). The main footprint emission feature covers an area of $5 \times 10^5 \text{ km}^2$ at Jupiter's atmosphere (Grodent et al., 2009), corresponding to a region 8–20 R_G wide in Ganymede's orbital plane ($R_G = 2,634 \text{ km}$ is Ganymede's radius). This region is significantly larger than the diameter of Ganymede due to Ganymede's own magnetosphere providing a factor of ~ 10 larger obstacle to the plasma flow and enhancing the size of its interaction region with Jupiter's magnetospheric plasma (Jia et al., 2008; Paty et al., 2008; Saur et al., 2013). Accounting for the footprint area, the average emitted power over the footprint is $0.4\text{--}13 \text{ mW/m}^2$. Assuming a 10% conversion efficiency from incident electron power to auroral emission power (Gérard & Singh, 1982; Grodent et al., 2001; Gustin et al., 2012), this corresponds to an average incident electron energy flux of $4\text{--}130 \text{ mW/m}^2$ for Ganymede's main auroral spot. Similar incident energy fluxes are inferred from a decade of Hubble Space Telescope observations of Ganymede's auroral footprint (Wannawichian et al., 2010). Its footprint tail fluxes are expected to follow an exponential decay in power as a function of angular separation from the main spot, with an *e*-folding distance of 11° (Bonfond, Saur, et al., 2017).

The Juno mission (Bolton et al., 2017) provides an unparalleled opportunity to investigate the acceleration processes driving Ganymede's complex auroral phenomena as the spacecraft directly transits flux tubes connected to this aurora. Magnetic field perturbations and the characteristics of the electrons responsible for causing emission in the Jovian atmosphere hold the clues to how this aurora is sustained. One auroral signature of particle acceleration/heating is the production of conics, where charged particle populations exhibit peak fluxes at oblique pitch angles (Klumpar, 1979). Observations of conics give insight into how electrons are accelerated on auroral field lines. Electron conics were first observed with the DE-1 spacecraft (Menietti & Burch, 1985) and have been associated with various auroral phenomena (Lysak 1993) such as parallel or perpendicular heating (e.g., Menietti & Burch, 1985; Temerin & Cravens, 1990) and low-frequency parallel electric fields (e.g., André & Eliasson, 1992; Lundlin et al., 1987; Thompson & Lysak, 1996). They have been observed frequently at Jupiter with Juno, likely driving the cyclotron maser instability, and are suggested to be due to inertial Alfvén waves (Louarn et al., 2018).

We focus on data taken when Juno transited magnetic field lines connected to Ganymede's auroral footprint tail, reporting on a variety of auroral phenomena such as broadband precipitating electrons, Alfvénic perturbations to the magnetic field, and up-going electron conics. First, we discuss the observation geometry and describe the correlation between remote UV and in situ fields and particle measurements necessary to link these measurements to the Ganymede footprint tail. We then discuss the specific details of the in situ measurements and conclude with a discussion.

2. Correlating Remote and In Situ Measurements

Ganymede orbits Jupiter at 15 Jovian radii (R_J), twice per orbit crossing Jupiter's current sheet that distends the magnetospheric magnetic field and makes it difficult to precisely trace magnetic field lines from its location to the Jovian atmosphere. Instead of correlating features in Juno plasma data to their equatorially mapped regions as done previously (e.g., Allegrini et al., 2017; Szalay et al., 2017), we link in situ

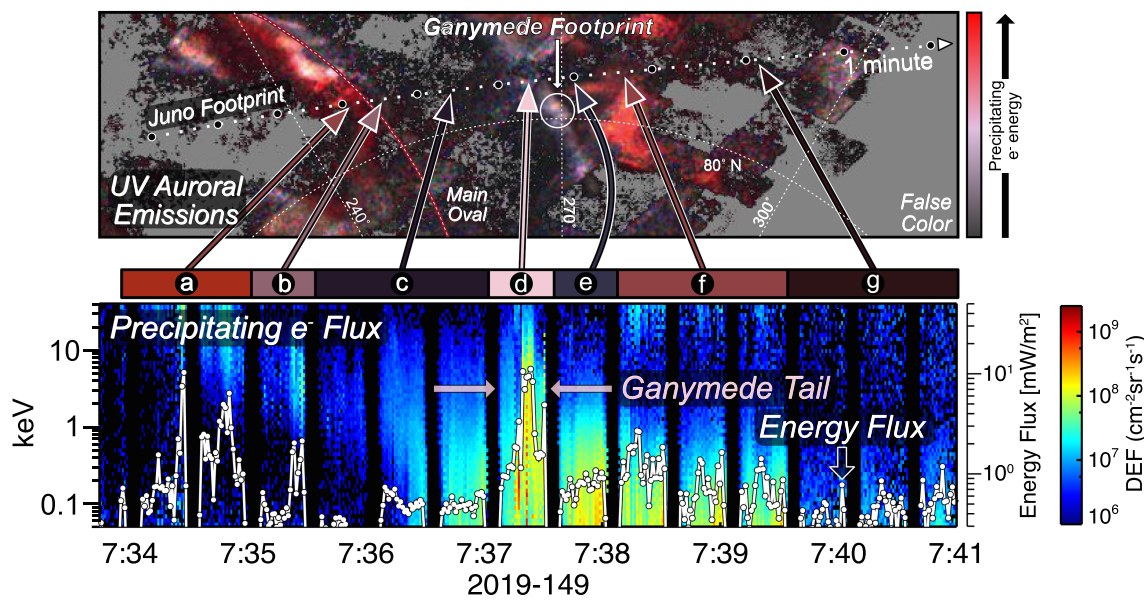


Figure 1. (top) UV false color of the auroral emissions near Juno's mapped magnetic footprint. Gray areas mark regions UVS either did not observe or registered no photons while viewing. Qualitatively, red features correspond to emissions deep in the atmosphere due to higher-energy precipitating electrons, while pink/white features correspond to higher-altitude emissions due to lower-energy incident electrons. (bottom) The color spectrogram shows JADE downward precipitating differential energy flux (DEF). The overlaid line shows energy flux (EF) within the loss cone, with the separate EF axis on the right of the spectrogram.

measurements of particles and fields with near-simultaneous UV images of the Jovian auroral emissions (e.g., Ebert et al., 2019; Gérard et al., 2019).

The top panel of Figure 1 shows a false-color UV image taken by Juno's Ultraviolet Spectrograph (UVS) (Gladstone et al., 2017) accumulated just prior to Juno's twentieth perijove over 10 min on 2019-149 (May 29) from 7:35:02 to 7:45:02 UTC (during which Ganymede has moved less than 1°). These colors can be qualitatively compared to precipitating electron energies observed in situ.

Juno's magnetic footprint is shown, traced from Juno's position to 400 km above the 1 bar level using the JRM09 field model (Connerney et al., 2018), which incorporates a current sheet model (Connerney et al., 1981). Juno's footprint moves from left to right in this image and the time between circles is 1 min. A nominal location for the main auroral oval is denoted with the solid red and dashed white line in the left half of the image. Ganymede's main auroral spot is the pink feature circled under the "Ganymede Footprint" label and arrow, with the tail extending up and left such that Juno's mapped footprint crossed it 8° downtail. Beginning on the left side of the image, Juno is transiting across Jupiter's polar region, where there is limited auroral emission coverage by UVS. Juno then encounters magnetic field lines connected to the main auroral oval, where the polar edge has a higher average energy incident to the atmosphere (a), shown in red, immediately followed by an auroral region with lower incident energy (b), shown in pink/maroon. Following this, it transits a region with very little auroral emission for about a minute (c). It then encounters Ganymede's footprint tail (d), which extends from the Ganymede MAW upward in this image. After this, it encounters a small region with low emission (e), followed by a region with high incident energy for about a minute and a half (f) and then encounters another region with low emission (g).

Uncertainties in the magnetic field mapping can lead to time shifts when comparing the emission thought to be underfoot to in situ particle and fields data. These effects can be more drastic when mapping from the northern hemisphere, due to the localized magnetic anomaly in this hemisphere (Grodent et al., 2008). Additionally, the latitude of Ganymede's auroral footprint can vary by 2° depending on current sheet properties (Grodent et al., 2009), adding to the complexities in determining its exact auroral mapping. Therefore, we do not compare Juno's location with field lines expected to map to Ganymede's orbit in the equatorial plane. Instead, we directly correlate emission features along Juno's mapped footprint to precipitating electron fluxes measured by the Jovian Auroral Distributions Experiment (JADE) (McComas et al., 2017), which exhibit similar temporal and energy structure. The bottom panel of Figure 1 shows JADE electron

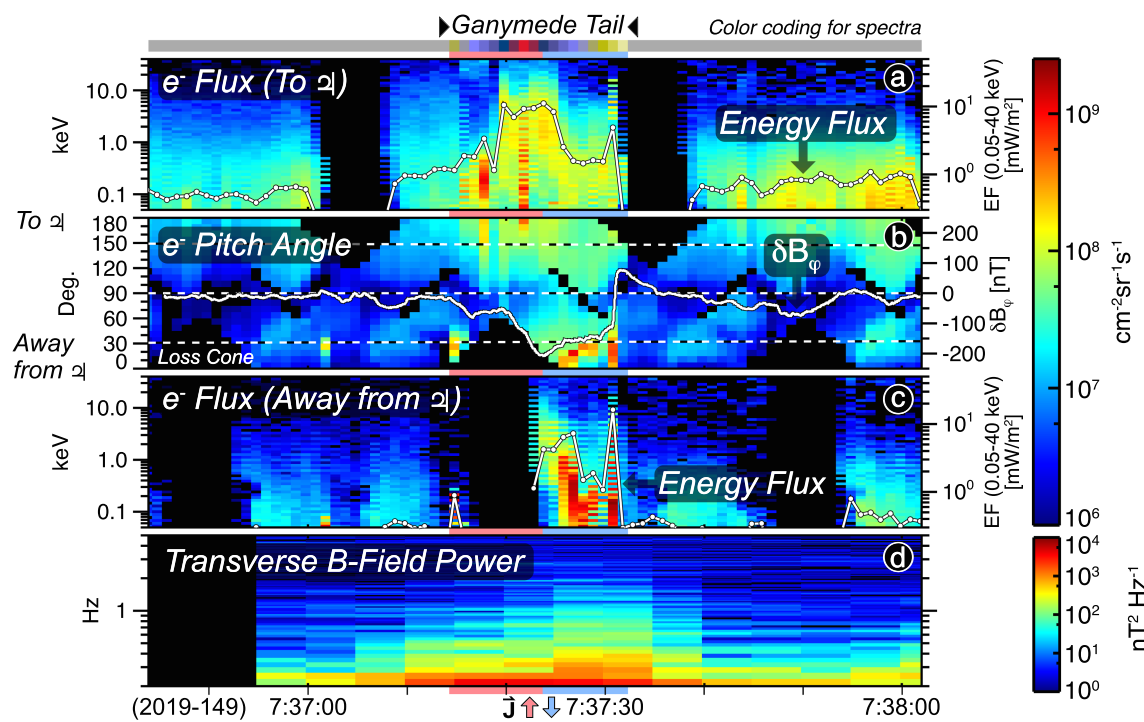


Figure 2. JADE and MAG data during the Ganymede footprint tail transit. Panels (a) and (c) show the downward and upward electron differential energy flux (DEF) within the loss cone, respectively. Precipitating energy flux is overlaid on these panels with its separate axes on the right of the spectrograms. Panel (b) shows electron pitch angles with δB_φ overlaid. Panel (d) shows the transverse B field power spectral densities. Red/blue bars indicate approximate upward/downward current regions inferred from MAG data.

differential energy fluxes (DEF) for precipitating electrons able to produce auroral emissions (observed in the loss cone) during this time. Pitch angles are calculated using the broadcast magnetic field onboard Juno (Connerney et al., 2017) at a cadence of 1 Hz. Overlaid on this spectrogram is the total downward precipitating energy flux (EF), described in more detail in section 3.

In region (a), JADE observes high-energy electrons, initially extending above JADE's energy range, then peaking in DEF at ~ 20 keV toward the end of (a). Subsequently, it measures a downward flux of electrons at lower average DEF energies of 2–20 keV in region (b). Region (c) is initially mostly void of downward electron fluxes, then transitions to a smaller low-energy component extending below 0.1 keV. In region (d), we observe a highly structured enhancement in downward energy flux, which is the focus of this study and will be shown in more detail in section 3. Region (e) returns to lower energy fluxes, similar to the second half of region (c). In region (f), JADE observed an enhancement in high-energy downward fluxes extending above ~ 10 keV. In region (g), JADE observes very low fluxes without appreciable structure.

Comparison of the temporal order of features seen as Juno transits this region by both UV and in situ electron measurements provides a high degree of correlation, both in average incident energy and feature duration. Given the high fidelity of correlation between the auroral emission image and downward energy flux, we attribute the enhancement observed in region (d) by JADE to the Ganymede footprint tail. Following this association, we describe the characteristics of auroral fields and particles connected to Ganymede's footprint tail in section 3.

3. In Situ Measurements

Figure 2 shows in situ measurements zoomed into region (d) from Figure 1, taken by Juno during 2019-149 from 7:36:44 to 7:38:02 UTC. The Ganymede footprint tail transit is identified as the period with enhanced fluxes in the center of this figure, from 7:37:14 to 7:37:42 and marked with the small color strip running

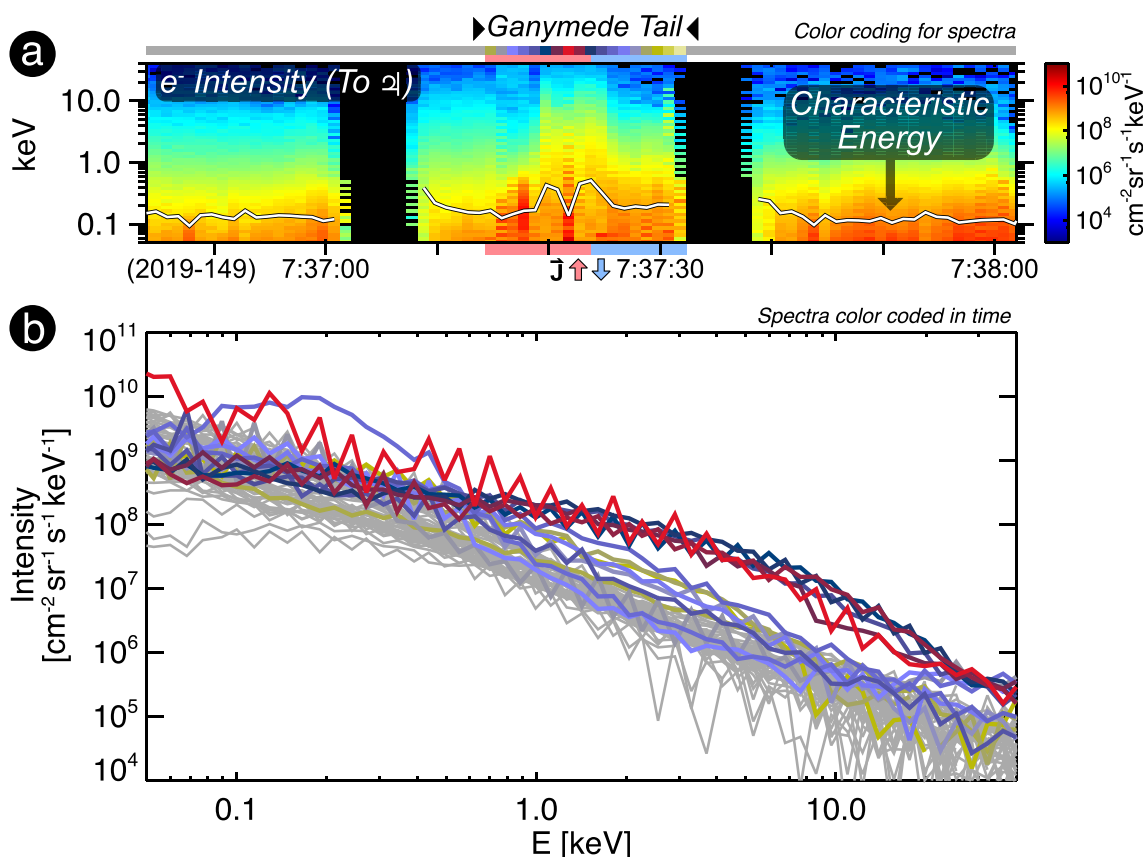


Figure 3. (a) Precipitating electron intensity spectrogram, with the characteristic energy from 0.05–40 keV overlaid. (b) Intensity for individual spectra, color coded by the bar at the top of (a).

along the top of the figure, where the colors indicate time from 7:37:22 and are used to identify spectra in Figure 3. Figure 2a shows the downward, precipitating electron differential energy flux, taken for measurements in the loss cone of 32° during this time (JRM09 model). Overlaid on this panel in white is the downward precipitating energy flux, which peaks at 11 mW/m^2 in the enhancement from 7:37:19 to 7:37:24. The downward energy flux is calculated as $EF = \pi \sum_i DEF_i \cdot E_i$, summing occurs over the JADE energies (subscript i), where π is the area-projection weighted size of the loss cone above Jupiter's atmosphere and E_i is the width of each energy bin following previous analyses (e.g., Mauk, Haggerty, Paranicas, Clark, Kollmann, Rymer, Mitchell et al., 2017). We calculate energy flux by summing from 50 eV to 40 keV. Since the fluxes above 40 keV are very near the noise floor, their omission does not substantially affect the analysis in this study. Figure 2c shows the same type of information as the first panel, but for the fluxes moving away from Jupiter in the upward loss cone.

Figure 2b shows DEF electron pitch angles for the same energy range. The JADE electron sensors provide 240° of azimuthal coverage (perpendicular to Juno's spin axis) and can electrostatically deflect up to 35° above/below Juno's spin plane to track the magnetic field direction. The missing 120° of azimuthal coverage leads to gaps in pitch angle, shown as the triangular regions with no observed fluxes in the second panel. At the onset of the identified Ganymede footprint tail transit (7:37:14), a short-duration electron conic is observed, peaking at around 30° . There is also a similar feature before the transit at 7:37:00. From 7:37:15 to 7:37:25, strong downward fluxes are observed, peaking in flux within the loss cone at 7:37:17 and 7:37:21. From 7:37:25 to 7:37:27, Juno encounters an upward beam that transitions to an electron conic from 7:37:27 to 7:37:29 with increasing peak pitch angle. The conic diminishes for a single time step (1 s) and an intense upgoing electron flux is observed at 7:37:30 spread more broadly in pitch angle, but also dominantly contained in the upgoing loss cone.

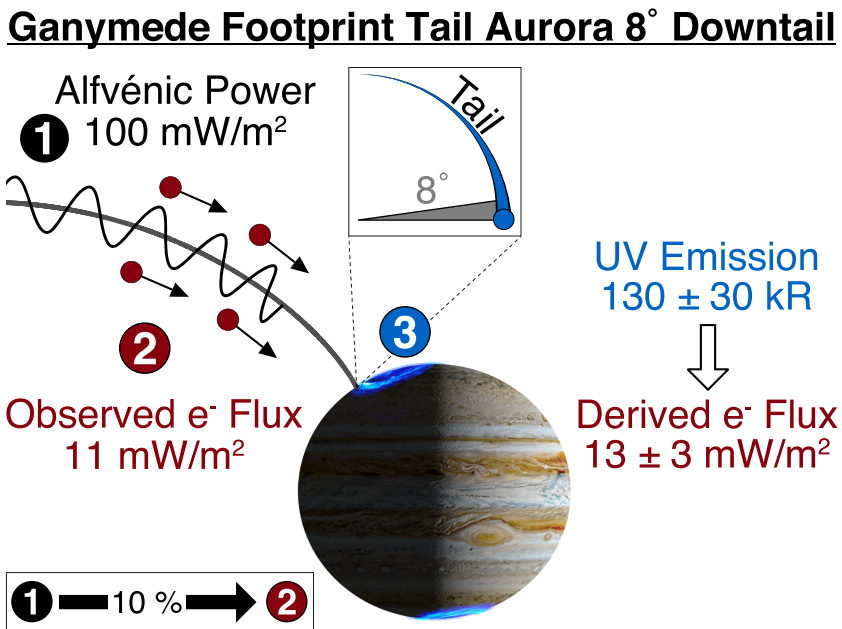


Figure 4. Summary schematic of the auroral processes involved in sustaining Ganymede's footprint tail aurora 8° downtail. Juno observations are consistent with a 10% efficiency coupling Alfvénic power to electron acceleration.

Overlaid on Figure 2b are background-subtracted magnetic field fluctuations in the azimuthal component (B_ϕ in System III coordinates), smoothed over 0.3 s to remove high-frequency fluctuations. The fluctuations are extracted from Juno magnetic field vector observations after removing the planetary magnetic field by subtracting the JRM09 model (Kotsiaros et al., 2019). Fluctuations reaching magnitudes up to ~200 nT are readily apparent in the transverse components (perpendicular to the magnetic field direction) and the absence of analogous compressive fluctuations (supporting information Figure S1) indicate that the currents are mostly field aligned. The magnetic field structure in δB_ϕ is typical of a northern Alfvén wing crossing with negative δB_ϕ within the main wing and positive δB_ϕ outside of the main wing (e.g., Neubauer 1980; Saur et al., 1999; Saur et al., 2007). The lack of positive δB_ϕ around 7:37:15 could be due to the detailed geometry of the tail substructures with respect to Juno's crossing.

The directionality of the currents can be determined by their azimuthal component. Specifically, the sharp decrease in δB_ϕ around 7:37:20 followed by a gradual increase at 7:37:24 and a sharp increase around 7:37:30 suggest that Juno crossed a localized upward current (downward electron beam) followed by a downward current (upward electron beam) typical of the northern sub-Jovian Alfvén wing flank (Saur et al., 1999; Jacobsen et al. 2007). Figure 2d shows the power spectral densities of the transverse magnetic field fluctuations. Following previous analysis techniques (Gershman et al., 2019) by determining the RMS fluctuation power over the given interval and assuming the Alfvén speed is the speed of light in such a strong magnetic field, the total Poynting flux is calculated to be ~100 mW/m². The Waves instrument onboard Juno (Kurth et al., 2017) also observed enhancements in electric and magnetic field fluctuations coincident with the tail transit time identified here and support these directionalities (supporting information Figures S2–S4). The power in the magnetic field fluctuations residing in the noncompressional (transverse) component up to 5 Hz, together with the absence of compressive magnetic fluctuations, is consistent with the presence of a non-dispersive Alfvénic mode transmitting field-aligned currents.

Figure 3a shows the intensity (or differential number flux, the DEF divided by electron energy for each energy bin), along with characteristic energy for the precipitating electrons. The characteristic energy is calculated via $E_{\text{char}} = \sum_i I_i E_i / \sum_i I_i$ (e.g., Clark et al., 2018), where I is the intensity and the sum is performed over an energy range from 50 eV to 40 keV. The characteristic energy varies from ~0.1 to 0.5 keV in the peak downward flux region, with a dip at ~0.1 keV at the center of the feature. Figure 3b shows intensity spectra for all time steps in the top panel, color coded by the bar at the top of the figure. During the times around the

peak downward energy flux (blue/red), the electron spectra exhibit a broad energization above ~ 0.5 keV. There is no clear evidence for a peak in the intensity profile indicative of a quasi-static parallel potential structure. The “sawtooth” pattern in some of the spectra is an instrumental effect due to JADE observing rapidly evolving electron fluxes, that vary on time scales shorter than the 1 s it takes for JADE to sweep every other energy step through all available energies.

4. Discussion and Conclusions

Juno has provided the first in situ measurements of particles and fields in the Ganymede footprint tail. Magnetic field measurements indicate strong Alfvénic activity, with Poynting fluxes ~ 100 mW/m² that provide sufficient energy to power the Ganymede footprint tail aurora. The observed Alfvén waves can accelerate electrons into the Jovian atmosphere, where JADE observed precipitating electron energy fluxes peaking at 11 mW/m², $\sim 10\%$ of the available Poynting flux energy. The precipitating electrons observed by JADE are sufficient to generate the instantaneously measured auroral emission from the Ganymede footprint tail. UVS observed the main auroral spot (Main Alfvén Wing = MAW) and near-spot auroral tail at this time to have an average H₂ photon flux of 130 ± 30 kR in the region associated with the Ganymede footprint (within the circle pointed to with the arrow in Figure 1). This value was calculated by summing the brightness within the 155–162 nm spectral range and then multiplying by a factor of 8.1 to scale it to the entire H₂ Lyman and Werner bands UV spectrum (Bonfond et al., 2017), where the error bar is due to systematic uncertainties in the radiometric calibration (Gérard et al., 2019). The UV intensities correspond to a precipitating electron energy flux of 13 ± 3 mW/m² (Grodent et al., 2001; Gustin et al., 2012). These observed values are also fully consistent with the expected values at $\Delta\lambda_G = 8^\circ$ angular separation from the MAW of 2–63 mW/m², assuming the fluxes are $\sim 50\%$ of the value at the MAW with an *e*-folding distance of 11° (Bonfond, Saur, et al., 2017). Figure 4 summarizes these findings.

Before and after the Ganymede footprint tail transit, the downward electron intensity spectra were power law-like as a function of energy, monotonically decreasing with energy resembling a power law function and without substantial substructure in energy. During the period of largest downward energy flux, the intensities increased by roughly an order of magnitude, with broad enhancements in the range of 0.5 to 40 keV. These downward electron spectra are characteristic of broadband acceleration, similar to those observed throughout Jupiter’s main auroral (Mauk, Haggerty, Paranicas, Clark, Kollmann, Rymer, Bolton, et al., 2017) and polar region (Ebert et al., 2017) emissions, and do not exhibit peaked features associated with discrete acceleration. While the shape of these spectra is not easily approximated by any of the canonical analytic distributions, to compare with similar previous fits, we fit the spectra to a Kappa distribution [equation 3.12 of Livadiotis & McComas, 2013], which yielded Kappa values of $\kappa = 1.5 - 2.8$. A Kappa value of 2.4 was found to best fit the precipitating electron fluxes at Io (Bonfond et al., 2009) and is within the range of values reported in this study for Ganymede, suggesting similar acceleration processes are involved.

At 8° separation from the MAW, the emissions map to a distance of $\sim 60 R_G$ downstream in Ganymede’s equatorial plane. During this event, Ganymede is at 280° System III longitude, such that it is within the northern portion of Jupiter’s plasma sheet and near the peak emission longitude of $\sim 310^\circ$ (Grodent et al., 2009). The broad structure of the feature is also consistent with Ganymede’s MAW spot size. Mapping the width of the feature discussed here down to an auroral emission altitude of 400 km above the 1-bar level, it spans a distance of 660 km in Jupiter’s atmosphere (supporting information Table S1), consistent with high-resolution observations showing the MAW spot to be ~ 700 km wide (Mura et al., 2018). The auroral current system is also highly structured, where the sawtooth/checkerboard pattern observed by JADE suggests the electron fluxes are varying on local scales smaller than 50 km (the distance Juno transits locally in JADE’s 1 s sampling period).

During the transit, Juno crossed a current system with separate upward and downward current regions adjacent to each other and exhibiting small-scale structures. In addition to these small-scale variations, electron beams and conics are observed in the upward current region (Figure 2b). Since there is no corresponding downward beam during this time, and more importantly since this population is in the loss cone, the conic is not a reflected loss cone distribution and instead indicates heating and/or acceleration below the spacecraft’s altitude of $0.5 R_J$.

The up-going electron beam at 7:37:25 indicates that parallel acceleration occurs below the spacecraft's altitude of $0.5 R_J$. If this beam and adjacent conic are generated by similar acceleration mechanisms, the conic could also have been driven by parallel acceleration. Low-frequency parallel electric field fluctuations, such as those from Alfvén waves, have been found to be able to generate electron conics (André & Eliasson, 1992). There is a trend of increasing peak pitch angle and decreasing characteristic energy and total energy flux in this conic. If the beam and conic are all formed due to similar parallel electric field fluctuations, this could indicate the acceleration region is getting further from Jupiter (closer to Juno) and decreasing in strength as Juno moves across the downward current region.

We observe a broad distribution of upgoing pitch angles at the edge of the downward current region, which suggests that acceleration occurs at a more dispersed range of altitudes near this boundary. The field-aligned upward electron beams in the loss cone in the downward current region could also generate conjugate auroral emissions in the southern hemisphere. However, if a similar acceleration process is occurring in the southern hemisphere, the lack of a downgoing conic in the upward current regions suggests that the downward electron flux may be more locally accelerated, and not due to a conjugate acceleration near the southern ionosphere. The one-way transit time to travel between hemispheres is ~ 16 min for 50 eV and ~ 0.5 min for 40 keV electrons and Ganymede has moved less than 1° during the transit. If such a conjugate population exists, they could have been pitch angle scattered during this transit. Ganymede's auroral tail features are also observed to be patchy and highly structured (Mura et al., 2018); therefore, it is possible that the features discussed in this study are a consequence of where Juno has crossed this patchy tail. Additionally, there is no evidence for a bifurcated tail like that intermittently observed for Io (Mura et al., 2018; Szalay et al., 2018).

While this study is focused on the electrons responsible for generating the auroral tail, there is some indication of proton acceleration (Figure S2), similar to that observed during the Io footprint tail transits (Szalay et al., 2019). Unfortunately, JADE does not have complete ion pitch angle coverage through this observation. Future studies could compare these accelerated protons to those accelerated in the Io footprint tail aurora, particularly on how the source of available protons and the Alfvén reflection scheme through the plasma sheet differs compared to the Io torus. Additionally, comparisons could be made between Io's and Ganymede's signatures in the high-energy component, where energetic proton depletions have been observed connected to Io's footprint tail aurora (Paranicas et al., 2019).

By simultaneously comparing observations of the Alfvén waves responsible for electron acceleration, the precipitating electrons they accelerate, and the auroral emissions those electrons produce, we confirm that Ganymede's footprint tail is sustained primarily by Alfvénic acceleration processes. Together with the finding that Io's footprint tail is also sustained primarily by similar processes (Bonfond et al., 2009; Hess et al. 2010; Szalay et al., 2019; Gershman et al., 2019; Damiano et al., 2019), Alfvénic acceleration appears to be a characteristic feature in Jupiter's moon-magnetosphere interactions and further bolsters the conclusion that broadband acceleration processes are dominant in Jupiter's aurorae (Mauk, Haggerty, Paranicas, Clark, Kollmann, Rymer, Bolton, et al., 2017; Saur et al., 2018). Saturn's moon Enceladus also exhibits similar auroral acceleration (Sulaiman et al., 2018); hence, similar processes are operating at multiple outer planets. By extension, Alfvénic acceleration is likely a more universal process applicable to similar interactions at other exoplanet-moon systems (Bonfond, Saur, et al., 2017; Saur et al., 2013).

Acknowledgments

The authors would like to thank the many JADE and Juno team members that made these observations possible. We thank V. Hue for producing the footprint prediction calculations. The JNO-J/SW-JAD-3-CALIBRATED-V1.0 data set was obtained from the Planetary Data System (PDS) at this site (<https://pds.nasa.gov/>). Data used in this manuscript can be found at <https://pubdata.space.swri.edu/look/0/88f58f56-36d3-4237-847e-54cb0c2fdad2>. We acknowledge the Juno's NASA Contract 699041X.

References

- Allegrini, F., Bagenal, F., Bolton, S., Connerney, J., Clark, G., Ebert, R. W., et al. (2017). Electron beams and loss cones in the auroral regions of Jupiter. *Geophysical Research Letters*, 44, 7131–7139. <http://doi.org/10.1002/2017GL073180>
- André, M., & Eliasson, L. (1992). Electron acceleration by low frequency electric field fluctuations—Electron conics. *Geophysical Research Letters*, 19(11), 1073–1076. <http://doi.org/10.1029/92GL01022>
- Bolton, S. J., Lunine, J., Stevenson, D., Connerney, J. E. P., Levin, S., Owen, T. C., et al. (2017). The Juno mission. *Space Science Reviews*, 213 (1–4), 5–37. <http://doi.org/10.1007/s11214-017-0429-6>
- Bonfond, B., Gladstone, G. R., Grodent, D., Greathouse, T. K., Versteeg, M. H., Hue, V., et al. (2017). Morphology of the UV aurorae Jupiter during Juno's first perijove observations. *Geophysical Research Letters*, 44, 4463–4471. <http://doi.org/10.1002/2017GL073114>
- Bonfond, B., Grodent, D., Badman, S. V., Saur, J., Gérard, J.-C., & Radioti, A. (2017). Similarity of the Jovian satellite footprints: Spots multiplicity and dynamics. *Icarus*, 292, 208–217. <http://doi.org/10.1016/j.icarus.2017.01.009>
- Bonfond, B., Grodent, D., Gérard, J.-C., Radioti, A., Dols, V., Delamere, P. A., & Clarke, J. T. (2009). The Io UV footprint: Location, inter-spot distances and tail vertical extent. *Journal of Geophysical Research*, 114, A07224. <http://doi.org/10.1029/2009JA014312>
- Bonfond, B., Grodent, D., Gérard, J.-C., Radioti, A., Saur, J., & Jacobsen, S. (2008). UV Io footprint leading spot: A key feature for understanding the UV Io footprint multiplicity? *Geophysical Research Letters*, 35, L05107. <http://doi.org/10.1029/2007GL032418>

- Bonfond, B., Hess, S., Bagenal, F., Gérard, J. C., Grodent, D., Radioti, A., et al. (2013). The multiple spots of the Ganymede auroral footprint. *Geophysical Research Letters*, 40, 4977–4981. <http://doi.org/10.1002/grl.50989>
- Bonfond, B., Saur, J., Grodent, D., Badman, S. V., Bisikalo, D., Shematovich, V., et al. (2017). The tails of the satellite auroral footprints at Jupiter. *Journal of Geophysical Research: Space Physics*, 122, 7985–7996. <http://doi.org/10.1002/2017JA024370>
- Clark, G., Tao, C., Mauk, B. H., Nichols, J., Saur, J., Bunce, E. J., et al. (2018). Precipitating electron energy flux and characteristic energies in Jupiter's main auroral region as measured by Juno/JEDI. *Journal of Geophysical Research: Space Physics*, 123, 7554–7567. <https://doi.org/10.1029/2018JA025639>
- Clarke, J. T., Ajello, J., Ballester, G., Ben Jaffel, L., Connerney, J. E. P., Gérard, J.-C. et al. (2002). Ultraviolet emissions from the magnetic footprints of Io, Ganymede and Europa on Jupiter. *Nature*, 415(6), 997–1000.
- Connerney, J. E. P., Acuna, M. H., & Ness, N. F. (1981). Modeling the Jovian current sheet and inner magnetosphere. *Journal of Geophysical Research*, 86, 8370–8384.
- Connerney, J. E. P., Benn, M., Bjarno, J. B., Denver, T., Espley, J., Jorgensen, J. L., et al. (2017). The Juno magnetic field investigation. *Space Science Reviews*, 213(1–4), 39–138. <http://doi.org/10.1007/s11214-017-0334-z>
- Connerney, J. E. P., Kotsiaros, S., Oliversen, R. J., Espley, J. R., Joergensen, J. L., Joergensen, P. S., et al. (2018). A new model of Jupiter's magnetic field from Juno's first nine orbits. *Geophysical Research Letters*, 45, 2590–2596. <http://doi.org/10.1002/2018GL077312>
- Damiano, P. A., Delamere, P. A., Stauffer, B., Ng, C.-S., & Johnson, J. R. (2019). Kinetic simulations of electron acceleration by dispersive scale Alfvén waves in Jupiter's magnetosphere. *Geophysical Research Letters*, 46, 3043–3051. <https://doi.org/10.1029/2018GL081219>
- Ebert, R. W., Allegrini, F., Bagenal, F., Bolton, S. J., Connerney, J. E. P., Clark, G., et al. (2017). Spatial distribution and properties of 0.1–100 keV electrons in Jupiter's polar auroral region. *Geophysical Research Letters*, 44, 9199–9207. <http://doi.org/10.1002/2017GL075106>
- Ebert, R. W., Greathouse, T. K., Clark, G., Allegrini, F., Bagenal, F., Bolton, S. J., et al. (2019). Comparing electron energetics and UV brightness in Jupiter's northern polar region during Juno Perijove 5. *Geophysical Research Letters*, 46, 19–27. <http://doi.org/10.1029/2018GL081129>
- Gérard, J.-C., Bonfond, B., Mauk, B. H., Gladstone, G. R., Yao, Z. H., Greathouse, T. K., et al. (2019). Contemporaneous observations of Jovian energetic auroral electrons and ultraviolet emissions by the Juno spacecraft. *Journal of Geophysical Research: Space Physics*, 124, 8298–8317. <https://doi.org/10.1029/2019JA026862>
- Gérard, J.-C., & Singh, V. (1982). A model of energy deposition of energetic electrons and EUV emission in the Jovian and Saturnian atmospheres and implications. *Journal of Geophysical Research*, 87(A6), 4525–4532. <http://doi.org/10.1029/JA087iA06p04525>
- Gershman, D. J., Connerney, J. E. P., Kotsiaros, S., DiBraccio, G. A., Martos, Y. M., Viñas, A. F., et al. (2019). Alfvénic fluctuations associated with Jupiter's auroral emissions. *Geophysical Research Letters*, 46, 7157–7165. <https://doi.org/10.1029/2019GL082951>
- Gladstone, G. R., Persyn, S. C., Eterno, J. S., Walther, B. C., Slater, D. C., Davis, M. W., et al. (2017). The ultraviolet spectrograph on NASA's Juno mission. *Space Science Reviews*, 213(1–4), 447–473. <https://doi.org/10.1007/s11214-014-0040-z>
- Grodent, D. (2015). A brief review of ultraviolet auroral emissions on giant planets. *Space Science Reviews*, 187(1–4), 23–50. <https://doi.org/10.1007/s11214-014-0052-8>
- Grodent, D., Bonfond, B., Gérard, J. C., Radioti, A., Gustin, J., Clarke, J. T., et al. (2008). Auroral evidence of a localized magnetic anomaly in Jupiter's northern hemisphere. *Journal of Geophysical Research*, 113, A09201. <http://doi.org/10.1029/2008JA013185>
- Grodent, D., Bonfond, B., Radioti, A., Gérard, J.-C., Jia, X., Nichols, J. D., & Clarke, J. T. (2009). Auroral footprint of Ganymede. *Journal of Geophysical Research*, 114, A07212. <http://doi.org/10.1029/2009JA014289>
- Grodent, D., Waite, J. H. J., & Gérard, J.-C. (2001). A self-consistent model of the Jovian auroral thermal structure. *Journal of Geophysical Research*, 106(A), 12933–12952. <http://doi.org/10.1029/2000JA900129>
- Gustin, J., Bonfond, B., Grodent, D., & Gérard, J. C. (2012). Conversion from HST ACS and STIS auroral counts into brightness, precipitated power and radiated power for H2 giant planets J. *Journal of Geophysical Research*, 117, A07316. <http://doi.org/10.1029/2012JA017607>
- Jacobsen, S., Neubauer, F. M., Saur, J., & Schilling, N. (2007). Io's nonlinear MHD-wave field in the heterogeneous Jovian magnetosphere. *Geophysical Research Letters*, 34, L10202. <http://doi.org/10.1029/2006GL029187>
- Hess, S. L. G., Delamere, P. A., Dols, V., Bonfond, B., & Swift, D. (2010). Power transmission and particle acceleration along the Io flux tube. *Journal of Geophysical Research*, 115(A), A06205. <http://doi.org/10.1029/2009JA014928>
- Jia, X., Walker, R. J., Kivelson, M. G., Khurana, K. K., & Linker, J. A. (2008). Three-dimensional MHD simulations of Ganymede's magnetosphere. *Journal of Geophysical Research*, 113, A06212. <http://doi.org/10.1029/2007JA012748>
- Klumpp, D. M. (1979). Transversely accelerated ions - An ionospheric source of hot magnetospheric ions. *Journal of Geophysical Research*, 84(A8), 4229–4237. <http://doi.org/10.1029/JA084iA08p04229>
- Kotsiaros, S., Connerney, J. E. P., Clark, G., Allegrini, F., Gladstone, G. R., Kurth, W. S., et al. (2019). Birkeland currents in Jupiter's magnetosphere observed by the polar-orbiting Juno spacecraft. *Nature Astronomy*, 3(10), 904–909. <http://doi.org/10.1038/s41550-019-0819-7>
- Kurth, W. S., Hospodarsky, G. B., Kirchner, D. L., Mokrzycki, B. T., Averkamp, T. F., Robison, W. T., et al. (2017). The Juno waves investigation. *Space Science Reviews*, 213(1–4), 347–392. <http://doi.org/10.1007/s11214-017-0396-y>
- Livadiotis, G., & McComas, D. J. (2013). Understanding kappa distributions: A toolbox for space science and astrophysics. *Space Science Reviews*, 175(1–4), 183–214. <http://doi.org/10.1007/s11214-013-9982-9>
- Louarn, P., Allegrini, F., McComas, D. J., Valek, P. W., Kurth, W. S., André, N., et al. (2018). Observation of electron conics by Juno: Implications for radio generation and acceleration processes. *Geophysical Research Letters*, 45, 9408–9416. <http://doi.org/10.1029/2018GL078973>
- Lundlin, R., Eliasson, L., Hultqvist, B., & Stasiewicz, K. (1987). Plasma energization on auroral field lines as observed by the Viking spacecraft. *Geophysical Research Letters*, 14(4), 443–446. <http://doi.org/10.1029/GL014i004p00443>
- Lysak, R. L. (1993). Generalized model of the ionospheric Alfvén resonator. *Auroral Plasma Dynamics*. (1993), 80, 121–128. <http://doi.org/10.1029/GM080p0121>
- Mauk, B. H., Haggerty, D. K., Paranicas, C., Clark, G., Kollmann, P., Rymer, A. M., et al. (2017). Discrete and broadband electron acceleration in Jupiter's powerful aurora. *Nature*, 549(7670), 66–69. <http://doi.org/10.1038/nature23648>
- Mauk, B. H., Haggerty, D. K., Paranicas, C., Clark, G., Kollmann, P., Rymer, A. M., et al. (2017). Juno observations of energetic charged particles over Jupiter's polar regions: Analysis of monodirectional and bidirectional electron beams. *Geophysical Research Letters*, 44, 4410–4418. <http://doi.org/10.1002/2016GL072286>
- McComas, D. J., Alexander, N., Allegrini, F., Bagenal, F., Beebe, C., Clark, G., et al. (2017). The Jovian auroral distributions experiment (JADE) on the Juno mission to Jupiter. *Space Science Reviews*, 213(1–4), 547–643. <http://doi.org/10.1007/s11214-013-9990-9>
- Menietti, J. D., & Burch, J. L. (1985). "Electron conic" signatures observed in the nightside auroral zone and over the polar cap. *Journal of Geophysical Research*, 90(A6), 5345–5353. <http://doi.org/10.1029/JA090iA06p05345>

- Mura, A., Adriani, A., Connerney, J. E. P., Bolton, S., Altieri, F., Bagenal, F., et al. (2018). Juno observations of spot structures and a split tail in Io-induced aurorae on Jupiter. *Science*, 361(6404), 774–777. <http://doi.org/10.1126/science.aat1450>
- Neubauer, F. M. (1980). Nonlinear standing Alfvén wave current system at Io - Theory. *Journal of Geophysical Research*, 85(A3), 1171–1178. <http://doi.org/10.1029/JA085iA03p01171>
- Paranicas, C., Mauk, B. H., Haggerty, D. K., Clark, G., Kollmann, P., Rymer, A. M., et al. (2019). Io's effect on energetic charged particles as seen in Juno data. *Geophysical Research Letters*, 46, 13615–13620. <http://doi.org/10.1029/2019GL085393>
- Paty, C., Paterson, W., & Winglee, R. (2008). Ion energization in Ganymede's magnetosphere: Using multifluid simulations to interpret ion energy spectrograms. *Journal of Geophysical Research*, 113, A06211. <http://doi.org/10.1029/2007JA012848>
- Saur, J., Grambusch, T., Duling, S., Neubauer, F. M., & Simon, S. (2013). Magnetic energy fluxes in sub-Alfvénic planet star and moon planet interactions. *Astronomy and Astrophysics*, 552, A119. <http://doi.org/10.1051/0004-6361/201118179>
- Saur, J., Janser, S., Schreiner, A., Clark, G., Mauk, B. H., Kollmann, P., et al. (2018). Wave-particle interaction of Alfvén waves in Jupiter's magnetosphere: Auroral and magnetospheric particle acceleration. *Journal of Geophysical Research: Space Physics*, 123, 9560–9573. <https://doi.org/10.1029/2018JA025948>
- Saur, J., Neubauer, F. M., & Schilling, N. (2007). Hemisphere coupling in Enceladus' asymmetric plasma interaction. *Journal of Geophysical Research*, 112, A11209. <http://doi.org/10.1029/2007JA012479>
- Saur, J., Neubauer, F. M., Strobel, D. F., & Summers, M. E. (1999). Three-dimensional plasma simulation of Io's interaction with the Io plasma torus: Asymmetric plasma flow. *Journal of Geophysical Research*, 104(A11), 25105–25126.
- Sulaiman, A. H., Kurth, W. S., Hospodarsky, G. B., Averkamp, T. F., Ye, S. Y., Menietti, J. D., et al. (2018). Enceladus auroral hiss emissions during Cassini's grand finale. *Geophysical Research Letters*, 45, 7347–7353. <http://doi.org/10.1029/2018GL078130>
- Szalay, J. R., Allegrini, F., Bagenal, F., Bolton, S., Clark, G., Connerney, J. E. P., et al. (2017). Plasma measurements in the Jovian polar region with Juno/JADE. *Geophysical Research Letters*, 44(14), 7122–7130. <http://doi.org/10.1002/2017GL072837>
- Szalay, J. R., Bagenal, F., Allegrini, F., Bonfond, B., Clark, G., Connerney, J. E. P., et al. (2019). Proton acceleration by Io's Alfvénic interaction. *Journal of Geophysical Research: Space Physics*, 125. <https://doi.org/10.1029/2019JA027314>
- Szalay, J. R., Bonfond, B., Allegrini, F., Bagenal, F., Bolton, S., Clark, G., et al. (2018). In situ observations connected to the Io footprint tail aurora. *Journal of Geophysical Research: Planets*, 123, 3061–3077. <https://doi.org/10.1029/2018JE005752>
- Temerin, M. A., & Cravens, D. (1990). Production of electron conics by stochastic acceleration parallel to the magnetic field. *Journal of Geophysical Research*, 95(A4), 4285–4290. <http://doi.org/10.1029/JA095iA04p04285>
- Thompson, B. J., & Lysak, R. L. (1996). Electron acceleration by inertial Alfvén waves. *Journal of Geophysical Research*, 101(A), 5359–5370. <http://doi.org/10.1029/95JA03622>
- Wannawichian, S., Clarke, J. T., & Nichols, J. D. (2010). Ten years of Hubble Space Telescope observations of the variation of the Jovian satellites' auroral footprint brightness. *Journal of Geophysical Research*, 115, A02206. <https://doi.org/10.1029/2009JA014456>

Reference From the Supporting Information

- Kolmašová, I., Imai, M., Santolík, O., Kurth, W. S., Hospodarsky, G. B., Gurnett, D. A., et al. (2018). Discovery of rapid whistlers close to Jupiter implying lightning rates similar to those on Earth. *Nature Astronomy*, 2(7), 544–548. <http://doi.org/10.1038/s41550-018-0442-z>